OXFORD UNIVERSITY PRESS Journal of Plankton Research

Impact of appendicularians on detritus and export fluxes: a model approach at DyFAMed site

Journal:	*Journal of Plankton Research*
Manuscript ID:	JPR-2010-214.R2
Manuscript Type:	Original Article
Date Submitted by the Author:	22-Nov-2010
Complete List of Authors:	Berline, Léo; LOV, LOV stemmann, Lars; UPMC, LOV Vichi, Marcello; Istituto Nazionale di Geofisica e Vulcanologia (INGV), Centro Euro-Mediterraneo per i Cambiamenti Climatici (CMCC) Lombard, Fabien; Technical University of Denmark, Oceanography Section Gorsky, Gaby; CNRS, INSU
Keywords:	Zooplankton, Appendicularian, Larvacean, Detritus, Export, Model, Plankton functional type, Time series station

Impact of appendicularians on detritus and export fluxes: a model approach at DyFAMed site

Léo Berline[a], Lars Stemmann[a], Marcello Vichi[b,c], Fabien Lombard[d,e], Gabriel Gorsky[a]

[a]*Laboratoire d'Océanographie de Villefranche (LOV), Station Zoologique-BP 28, 06234 Villefranche-sur-mer, France,*
[b]*Centro Euro-Mediterraneo per i Cambiamenti Climatici (CMCC), Via Aldo Moro 44, 40127 Bologna. Italy*
[c]*Istituto Nazionale di Geofisica e Vulcanologia (INGV), Via Aldo Moro 44, 40127 Bologna. Italy*
[d]*Technical University of Denmark, National Institute of Aquatic Resources, Oceanography Section, Charlottenlund, Denmark*
[e]*Laboratoire d'Océanographie Physique et Biogéochimique (LOPB), Université de la Méditerranée (Aix-Marseille II), LOPB - UMR 6535 Campus de Luminy Case 901, F-13288 MARSEILLE Cedex 9, FRANCE*

Abstract:
So far, the role of appendicularians role in the biogeochemical cycling of organic matter has been largely overlooked. Appendicularians represent only a fraction of total mesozooplankton biomass, however these ubiquitous zooplankters have very high filtration and growth rates compared to copepods, and produce numerous fecal pellets and filtering houses contributing to export production by aggregating small marine particles. To study their quantitative impact on biogeochemical flux, we have included this group in the Biogeochemical Flux Model (BFM), using a recently developed ecophysiological model. One dimensional annual simulations of the pelagic ecosystem including appendicularians were conducted with realistic surface forcing for the year 2000, using data from the DyFAMed open ocean station. The appendicularian grazing impact was generally low, but appendicularians increased detritus production by 8% and export production by 55% compared to a simulation without appendicularians. Therefore current biogeochemical models lacking appendicularians probably under, or misestimate the detritus and export production by omitting the pathway from small sized plankton to fast sinking detritus. Detritus production and export rates are 60% lower than estimates from mesotrophic sites, showing that appendicularians' role is lower but still significant in oligotrophic environments. The simulated annual export at 200 m exceeds sediment trap values by 44%, suggesting an intense degradation during the sinking of appendicularian detritus, supported by observations made at other sites. Thus degradation and grazing of appendicularian detritus need better quantification if we are to accurately assess the role of appendicularia in export flux.

Keywords:

Zooplankton *, Appendicularian *, Larvacean *, Detritus *, Export *, Model *, Plankton functional type *, Time series station *

Introduction

In the world ocean, appendicularians are often the most abundant mesozooplankton group after copepods (Gorsky and Fenaux 1998). According to Hopcroft et al (1998), "*Appendicularian (also*

named larvacean) impact on phytoplankton communities may be substantial (Alldredge, 1981; Nakamura et al, 1997), in part because their specific filtration rates may be greater than that of other metazoans (e.g. copepods, Alldredge and Madin, 1982). Their importance as linkages between the microbial and classical food webs (Urban et al, 1992), and significance in terms of carbon flux (Urban et al., 1993), may also be underappreciated". This lack of recognition is likely due to lower biomass compared to copepods, the difficulty of in situ investigations, and their fragility, resulting in high mortality, damage and stress during net sampling. Although their biomass is low compared to copepods, their physiological rates are significantly higher, up to one order of magnitude higher (López-Urrutia et al 2003). Appendicularian fecal pellet production, mortality, respiration, and excretion rates are also significantly greater that those of copepods (Sato et al 2005, Dagg and Brown 2005a; Lombard et al 2005, 2009a).

A unique characteristic of appendicularians is their external filtering apparatus, the filter house, that sieves and concentrates a wide range of particle sizes from 0.2 – 30 µm, thus capturing organisms from bacteria to microplankton (Flood et al 1992; Gorsky and Fenaux, 1998; Lombard et al 2010). These mucous houses get clogged as they retain a fraction of the filtered particles. In order to maintain their filtering capability, appendicularians continuously secrete and discard filtering houses, generating a large, carbon-rich detritus flux in addition to fecal pellets.

Thus appendicularians deserve attention as an important component of the flux in the mesozooplankton compartment. However, in most models used to study biogeochemical fluxes in the marine ecosystem, the mesozooplankton compartment consists mainly of copepods (e.g. Fasham 1990). In the last decades, food web models have been improved and rendered more realistic by splitting phytoplankton, and to a lesser extent zooplankton, into functional or size class groups (e.g. Baretta et al, 1995 ; Aumont et al 2003 ; Le Quéré et al 2005 ; Vichi et al 2007). But within zooplankton, the mesozooplankton component is still parameterized typically to represent only copepods. Le Quéré et al (2005) proposed distinguishing appendicularians as a separate functional type, but grouped them in a large macrozooplankton group of euphausiids, pteropods and salps, organisms with very different physiology and life cycles.

In recent years, while being neglected in ecosystem models, knowledge of appendicularian seasonal cycles, ecology, physiology and metabolism has advanced significantly from in situ observations and laboratory experiments. Models have been developed to simulate individual growth, life cycle, food uptake, respiration, fecal pellets and house production (Touratier et al 2003; López-Urrutia et al., 2003; Alldredge, 2005; Aksnes et al. 2006; Lombard et al 2009b). However, these individual-

based models lack the food web dynamics, i.e. the interaction of appendicularian prey and predators, and are restricted to a single life cycle of a few days.

To our knowledge, there has been only a single attempt (Andersen et al 1987) to include appendicularians in a food web model. The goal of Andersen et al (1987) was to adequately model herbivore dynamics over a 40 day period in a controlled experiment, though at that time ecophysiological knowledge of appendicularians was largely incomplete. Here, we present work representing a step towards the integration of appendicularians within state-of-the-art, spatially-resolved biogeochemical models. A biomass-based set of parameterizations derived from the individual-based model of Lombard et al (2009b) was included as an additional module in the Biogeochemical Flux Model (BFM, Vichi et al 2007) to study appendicularian impact on grazing, detritus production, export and remineralization rates at an annual scale under realistic conditions. The model was parameterized for the DyFAMed station in the North West Mediterranean, where comprehensive data on biogeochemistry and zooplankton are available for validation (Marty, 2002). This station has mesotrophic conditions during the winter-early spring bloom, followed by oligotrophic conditions in summer.

The article is structured as follows: the model and data used for initialization and validation are first described. Then we present the results of comparisons: 1) between annual cycles with and without appendicularians, 2) examining the impact of the mortality formulation, and the sensitivity to various appendicularian species, input parameters and forcing conditions. We then end with a comparative discussion with other study sites and draw conclusions.

Method

The coupled physical-biogeochemical model

A coupled hydrodynamical-biological model was implemented to describe the temporal changes in temperature, diffusion, and concentration of biogeochemical tracers in a one-dimensional vertical water column.

The software GOTM (Generalized Ocean Turbulence Model; Burchard et al 1999, http://www.gotm.net) computes changes in temperature and vertical diffusion coefficient forcing

the biogeochemical model. The biogeochemical model has a feedback effect on physics through light attenuation by phytoplankton. GOTM has been coupled to biogeochemical models in several studies (e.g. Burchard et al 2005; Neumann et al 2002).

The biogeochemical model is BFM (Biogeochemical Flux Model, http://bfm.cmcc.it; Vichi et al 2007), successor to the ERSEM model (Baretta-Bekker et al 1997). BFM has been successfully used in global studies (e.g. Vichi and Masina 2009) and in the Mediterranean region (Carniel et al., 2007; Polimene et al., 2007; Lazzari et al., 2010). It describes the dynamics of the lower trophic levels of the marine ecosystem and associated element fluxes (C, N, P, Si, O2, Fe). BFM is modular, meaning that biological compartments can be turned on and off, so that food web complexity is scaled to the aim of the study. In the present set up designed for DyFAMed, the model included bacterioplankton, three size classes of phytoplankton (microphytoplankton (diatoms), nanophytoplankton (nanoflagellates) and picophytoplankton) and three size classes of zooplankton (heterotrophic nanoflagellates termed HNAN hereinafter, microzooplankton and copepods), plus appendicularians (Fig. 1).

The appendicularian module was derived from the equations described in Lombard et al (2009b), with some simplifications. These simplifications were needed to turn the individual-based model into a biomass-based model, suitable for coupling with the hydrodynamic model at the annual scale. Appendicularians are represented in bulk biomass, passively transported as the copepod functional group. Allometric relationships for filtration and respiration have been neglected (implies allometric coefficient = 1 instead of 0.9 and 0.75 respectively). The food trapped in the house is directly released as slow and fast sinking detritus into the water column (i.e. houses are discarded instantaneously instead of 0.5-1 per hour). All biomass is composed of structural biomass (no gonad fraction). The adequacy of these simplifications was first tested with zero dimensional model experiments reproducing appendicularian growth in laboratory cultures with satisfactory results.

Mortality needed to be considered in order to study time scales much greater than the appendicularian life cycle. A constant mortality rate was applied, taking into account adult mortality and egg hatching mortality (respectively 0.1 d-1 and 50%, Lombard, unpub. results). In addition to this linear mortality term due to life history, a density dependent mortality term (Edwards and Brindley 1999; Edwards and Yool, 2000) was used to represent predation by higher trophic levels, namely fish larvae or gelatinous carnivores (Gorsky and Fenaux 1998; Fyhn et al 2005). As in situ mortality rates are unknown, mortality parameters were set from model trials. We further assessed the impact of the rate choices by simulations without considering any mortality (see simulation set

up).

Corresponding with their known prey size range, appendicularians feed on bacteria, HNAN, microzooplankton and the phytoplankton compartment (Flood et al. 1992), with a preference for picophytoplankton and HNAN (see parameters in appendix). Appendicularians are preyed upon by copepods (especially egg and juvenile stages of appenducularians, Sommer et al 2003; Stibor et al 2004; López-Urrutia et al 2004). As a first step in representing diversity in detritus size and sinking velocity, the detritus pool was divided into slow and fast sinking components and a fast appendicularian component. Slow detritus, sinking at 1.5 m/day, is produced by phytoplankton, bacteria (mortality), HNAN and microzooplankton (mortality, excretion), copepods and appendicularians (excretion and egestion). Fast detritus, produced by the copepods as fecal pellets, was set to sink at 5.0 m/day. Although fecal pellets may sink faster than 5 m/day (e.g. 70-171 m/day, Bienfang 1980), this low value has been demonstrated to be necessary to keep enough organic matter in the surface layer in a one-dimensional model (Lacroix and Nival 1998). Appendicularian detritus (fecal pellets and 85% of the houses, Lombard and Kiørboe, 2010) was set at 40 m/day, which is in the lower range of estimates from Lombard and Kiørboe (2010) and Gorsky et al (1984).

The general equation for the time rate of change of appendicularian carbon biomass is reported here according to the notation by Vichi et al. (2007):

$$\left.\frac{\partial App}{\partial t}\right|_{bio} = \sum_{X=preys} \left.\frac{\partial App}{\partial t}\right|_{X}^{flt} - \left.\frac{\partial App}{\partial t}\right|^{rsp} - \left.\frac{\partial App}{\partial t}\right|_{Det}^{rel} - \left.\frac{\partial App}{\partial t}\right|_{Det}^{mrt} - \left.\frac{\partial App}{\partial t}\right|_{Cop}^{prd} \quad (1)$$

The terms on the right hand side represent filtration, respiration, organic matter release to detritus, natural mortality and carbon losses due to predation.

Filtration depends on the carbon concentration of total available food

$$F = \sum_{X=preys} \delta_X X \quad (2)$$

where X is the carbon biomass of each prey item and δ_X the non-dimensional preference factor from 0 to 1 (see parameter table in appendix). The filtration rate for each prey category is written as a Holling type-II function with total food controlled by two parameters (see appendix), a maximum temperature-dependent filtration rate $f_0\ \theta^T_f$ and the half saturation food concentration K_F:

$$\left.\frac{\partial App}{\partial t}\right|_{X}^{flt} = \left(\frac{\delta_X X}{F}\right) f_0 \theta_f^T \frac{F}{F + K_F} App \qquad (3)$$

Respiration is assumed to be only metabolic, and parameterized as a linear function of temperature and a constant respiration rate with

$$\left.\frac{\partial App}{\partial t}\right|^{rsp} = f_r \theta_r^T App \qquad (4)$$

Only a portion of food items filtered in eq. (3) is ingested: a fraction β is directly released in the house and only a part η of the remainder is incorporated into biomass, while the fraction *1-η* is egested as fast-sinking fecal pellets Both β and η depend on food availability:

$$\beta = 1 - \beta_m \frac{F}{K_\beta + F} \qquad (5)$$

$$\eta = 1 - \eta_m \frac{F}{K_\eta + F} \qquad (6)$$

The loss rate to detritus is therefore partitioned in

$$\left.\frac{\partial App}{\partial t}\right|_{Det}^{rel} = \left[(1-\beta) + (1-\eta)\beta\right] \left.\frac{\partial App}{\partial t}\right|_{X}^{flt} \qquad (7)$$

where the first term is partly released in the water column as slow sinking detritus (a constant fraction ε=0.15, Lombard and Kiørboe, 2010) and the remainder stays trapped in the house and sinks as fast sinking detritus just like fecal pellets.

Natural mortality is parameterized as the sum of a linear term and a quadratic population-dependent term

$$\left.\frac{\partial App}{\partial t}\right|_{Det}^{mrt} = mApp + m_{dns} App^2 \qquad (8)$$

The internal C:N quota is assumed to be constant. The excess of nutrient or carbon in assimilated food is eventually computed and compared to the internal quota as proposed by Broekhuizen et al. (1995), then the remainder is excreted.

Predation by copepods in eq. (1) is written as in Vichi et al. (2007).

Validation data

The model was parameterized for the DyFAMed station, located in the central part of the Ligurian Sea, in the North West Mediterranean. The weak horizontal advection at DyFAMed allows one dimensional vertical studies of the ecosystem (see Raick et al 2005 for a review). This station was chosen as data were available to validate the model: temperature, salinity, nutrients, phytoplankton fluorescence and pigment composition data are available over the period 1991-2007 at a quasi monthly frequency, while microbial food web and mesozooplankton data are available for some specific periods (see http://www.obs-vlfr.fr/sodyf/). In year 2000, 11 samples with chlorophyll, pigments and nutrient concentrations are available. According to the chemotaxonomic classification of Vidussi et al (2001), nanophytoplankton dominated (46%) over microphytoplankton (33%) and picophytoplankton (16%) during year 2000. Mesozooplankton was sampled with WP2 vertical net tows (200 µm mesh) and mesozooplankton samples for taxonomic identification are available for the years 2006-2008.

The model-data linear fit was quantified with the Pearson correlation coefficient R.

The biomass of copepods and appendicularians was estimated from abundance and size measurements obtained from digitized images of the samples made with the ZooScan. The ZooScan is a laboratory instrument for digitization of fixed net samples developed at the Laboratoire d'Océanographie de Villefranche-sur-mer (Gorsky et al., 2010). The semi automatic recognition method is fully described in Gorsky et al (2010). From the sample image, all objects were automatically sorted into broad taxonomic groups through a supervised clustering technique. The results from the automatic sorting were manually checked by a taxonomist, and some groups were subdivided. Among appendicularians, *Oikopleura spp* and *Fritillaria spp* were distinguished, while copepods were pooled into one single group. We focused our study on *Oikopleura spp*, neglecting *Fritillaria spp* because the contribution of *Oikopleura* to export was shown to be dominant (Vargas et al 2002). Next, biomass was estimated. For copepods, the prosome length (L_P) was computed from a linear regression of the major axis length (L_M) measured by the imaging software ($L_P = 0.76\ L_M$, R^2=0.95). Length was converted to dry weight using Hay et al (1991), then converted to carbon with a carbon weight over dry weight ratio of 0.447 (Båmstedt 1986). For *Oikopleura* the trunk length was measured on 50 images (290±140 µm). Then the trunk length distribution was converted to weight distribution with the Sato et al (2004) relationship for *Oikopleura longicauda*, this species being the most abundant in summer (Fenaux 1961). Then the mean body carbon was computed as

the average weight distribution. The weight estimated from the Lombard et al (2009a) relationship for *O dioica* is similar (30% lower) to Sato et al (2004). Total mesozooplankton biomass data were also available for 2001-2002 (Gasparini et al 2004).

Simulations set up

The chosen model vertical resolution is 4 m, from the surface down to 200 m. Surface heat and momentum fluxes were computed by bulk formulae (Burchard et al 1999). The 6-hourly meteorological variables described in d'Ortenzio et al (2008) (wind at 10 m, air pressure, air temperature, dew point temperature, cloudiness) were used. The *tke* turbulence closure model was used as in Lacroix and Nival (1998) and Carniel et al (2007). To reduce model drifts and provide an adequate physical environment during the simulation, surface temperature was restored to in situ temperature with a fitted time scale of 27 hours. For simplicity and as reported in previous modeling studies (Raick et al 2005), we have assumed that nitrogen was the only limiting nutrient. Year 2000 was chosen to validate the model because of relatively comprehensive biological data and for comparison with Raick et al (2005). January 1st initial conditions for nitrate were taken from the year 2000 in situ data, while all other biological compartments were set to a constant value (0.1 mgC/m^3). 3 year simulations with the same annual surface forcing were run. After 2 years, physics and biology reached a steady state and only the 3rd year was analyzed. Through the model open bottom boundary, matter is lost by detritus sinking. To avoid depletion of the water column, nitrate was restored at the bottom to the annual average value (7.5 mmol/m^3). During winter, vertical mixing reaches the bottom and refuels the surface layer, so that the nutrient pre-bloom conditions are identical throughout the years.

As the appendicularian mortality term has an impact on slow detritus production and on the seasonal cycle of appendicularians, our choice of mortality rate partly determined the estimated detritus and export production. To quantify this effect, we conducted simulations with zero mortality, but with the biomass set to idealized analytical values for comparison with our simulations with mortality set. These simulations are called OFF (offline), while simulations including mortality are called FREE. The offline biomass used for simulations OFF (Fig. 4, heavy dashed line in the appendicularians panel) represents an idealized seasonal cycle with a minimum in winter and a maximum in summer, built from our 2006-2008 observations of abundance of *Oikopleura spp.* The vertical distribution follows the appendicularian prey field, as observed in the FREE simulations. The imposition of appendicularian biomass in the OFF simulation implies that at each time step the source-minus-sink term is zero, i.e. the net gain (or loss) computed by the

equations is virtually compensated by an external loss (or gain) so that biomass stays at the prescribed value. This external flux is computed during the simulation. It represents the 'offline mortality' term, not parameterized in the model.

Appendicularian model parameters were set to represent *O longicauda*, the commonest species in summer and fall at DyFAMed (Lombard et al 2010). For comparison, simulations were also run with parameters corresponding to the two other main species (*O dioica* and *O fusiformis*), using Lombard et al (2010) values.

First a simulation with no appendicularians (no-app) was validated over year 2000 against the available observations. Then the same simulation was repeated including appendicularians with mortality (app-free) to assess their impact on biomasses and fluxes. The OFF simulations were conducted to address (i) the influence of the mortality term, (ii) the role of two other appendicularian species and (iii) the sensitivity to biological parameters and nutrient pre-bloom conditions. OFF simulations were preferred over FREE for (ii) and (iii) because they provide flux estimates which are independent of the *a priori* chosen mortality rates. All simulation set-ups are summarized in Table 1.

Results

The net growth rate of modeled appendicularians differs from the other zooplankton compartments (Fig. 2). Because of their variable ingestion and assimilation efficiency, appendicularian growth saturates and decreases at food concentration higher than 100 mgC/m^3 (see equations in Appendix). Appendicularians have growth rates 2 to 3 times higher than copepods under nearly all conditions of food and temperature. They also have higher growth than microzooplankton at food concentrations between 25 and 150 mgC/m^3 and temperatures lower than 25°C. In contrast, they always have lower growth rates than HNAN.

The water column is deeply mixed in February and March (mixed layer depth greater than 200 m) and temperature is homogeneous and stable around 13°C for model and observations (Fig. 3). The spring stratification is correctly represented by the model, as well as summer stratification. The destratification starts in September in the model instead of October as found in the observations, causing the mixed layer depth to be slightly overestimated. The 5 m temperature follows the observations as expected from the imposition of a restoration term (Sec. 2) with a steady increase

from April to July, and a decrease after August.

For the sake of simplicity, model outputs and observations are compared as depth integrals over 0-200 m, except for bacteria, microzooplankton and HNAN which were sampled over 5-110 m (Fig. 4). HNAN and microzooplankton biomass are also pooled and discussed jointly from here on.

For the simulation without appendicularians, the biomass of the main components is in reasonable agreement with the monthly observations, (Fig. 4, dashed lines). R values are larger than 0.6 (0.6, 0.7, 0.9, 0.7 respectively for Chl, copepods, bacteria and microzooplankton+HNAN) except for nitrate and appendicularians (0.4 and 0.3 respectively). The spring bloom occurs in March, with simulated Chl at ca 120 mg/m^2, consistent with observations although the highest value observed in the available monthly sampling frequency is around 60 mg/m^2. A deep chlorophyll maximum (not shown) is simulated at about 60 m, agreeing with observations (Marty et al 2002). During the phytoplankton bloom, nitrate decreases steeply, but not as much as in the observations. In summer, nitrate stabilizes then decreases slowly in the model and observations. The microzooplankton+HNAN development immediately follows the phytoplankton bloom. Simulated microzooplankton+HNAN is low in winter, then peaks at ca. 1300 mg/m^2 in April-May, while observations range from ca 100 to 800 mgC/m^2. In April, copepod biomass builds up slowly, staying in the low range of observations that span from 0.5 to 5 gC/m^2. The high variability of these data is due to the addition of several years. Bacterial biomass is slightly underestimated, but in reasonable agreement with observations with a maximum in summer.

On an annual scale, net primary production (102 gC/m^2/yr, Table 2) is in the lower range of the estimations from in situ samples and from satellite estimates from other years (78 to 158 gC/m^2/yr, see Levy et al 1998, and 86-232 gC/m^2/yr for Marty and Chiaverini 2002). Annual export production (noted EP hereinafter, computed as the downward flux of detritus at 200 m depth) is also in agreement with observations (4.2 vs 4.5 gC/m^2/yr) for year 2000. The year 2000 value is similar to observations from other years (5 gC/m^2/yr in 1987-1988 and 4 gC/m^2/yr on average over 1987-1990, Miquel et al 1994, 1993).

The simulation with appendicularians (Fig. 4, solid lines) shows little difference in biomass compared to the simulation without appendicularians. The microzooplankton biomass compartment is the most reduced (-21% on annual average), especially in summer, while nitrate, copepod biomass is also slightly lower (-1%, -6% respectively) and bacteria, Chl slightly higher (+0.5%, +1% respectively). Appendicularian biomass stays very low in winter, then peaks in May at about

80 mgC/m^2 and decreases steeply until November. Appendicularian trends show one maximum of about 50 mgC/m^2 in June-July, but short peaks are also present in spring and fall. Appendicularian simulated biomass starts increasing in March, as soon as the phytoplankton bloom starts, but does not accumulate before May as winter biomass is too low.

The seasonal cycle of production and export fluxes for the simulation without appendicularians is shown in Fig. 5. Net primary production occurs mainly from March to July. Net secondary production (Fig. 5A) occurs from April to June for microzooplankton, April to July for copepods. Export production (EP, Fig. 5B) is distributed from April to August. In April, EP rises to 20-30 mgC/m^2/day in phase with the observations, peaks in June then decreases in July, consistent with observations (Miquel et al 1994). Then EP drops to a minimum in September and the smaller peak observed in November is not reproduced in the model. The two peaks of primary production (in April and May), only noticeable in the simulated slow detritus export, are present in the observed export. In winter, the observations show a low but non-negligible export of about 6 mgC/m^2/day, while the simulated export is slightly underestimated (4 mgC/m^2/day). The increase in fast detritus export follows copepod growth. The export peak is delayed compared to the surface production peak as detritus takes 20 to 40 days to sink from the production zone (approximately 0-100 m) to 200 m depth. The slow fraction contributes all year round to EP, since it is produced by all living groups (phytoplankton, microzooplankton+HNAN, bacteria and appendicularians). The fast-sinking fraction is mostly important during spring and summer, as it is only produced by copepods.

In contrast with their weak effect on the biomass of other groups, the contribution of appendicularians to export fluxes can be significant (Figs 6, 7 and Table 2). During the peak at the end of May (Fig. 6), at the rate of 60 mgC/m^2/day, their contribution to export is twice that of copepods, and higher than observations (see discussion below). The exported slow detritus fraction produced by appendicularians is negligible. Annually, appendicularians produce 7 gC/m^2/yr net production, compared to 28.4 gC/m^2/yr by microzooplankton and 19.0 gC/m^2/yr by copepods. Thus appendicularians represent only 12 % of zooplankton secondary production, however their ratio of annual production to biomass is the largest (394 against 67 for microzooplankton and 51 for copepods). Appendicularians represent 20% of fast detritus production. The fast detritus fraction dominates the total EP (82%), and appendicularians provide 2.4 gC/m^2/yr, i.e. 37% of total EP (fast and slow detritus export). Slow detritus production is dominated by copepods, phytoplankton and bacteria, with lower contributions from microzooplankton and appendicularians. The presence of appendicularians results in a slight reduction in primary production, secondary production by copepods and microzooplankton, and bacterial uptake by microzooplankton (Figs. 7 and 8).

Appendicularians also slightly increase the production of slow detritus (6%) but substantially (13%) increase the fast detritus production through their uptake of phytoplankton, bacteria, and to a lesser extent microzooplankton. The appendicularian contribution to ammonia production is of the same order of magnitude as that of copepods. Ammonia is partly produced by bacterial degradation of dissolved organic matter and detritus pools, but also by microzooplankton and copepod excretion. Additional simulations conducted with surface forcings from other years (1998 to 2004, not shown) indicate that the reported fluxes are weakly sensitive to the interannual variability in the physics, as the standard deviations of fluxes are generally lower than 10% of their mean value.

The role of mortality was specifically analyzed comparing the simulations FREE (app-free, parameterized mortality) and OFF (app-off, no mortality and prescribed biomass). The results are summarized in Table 2. The OFF simulation has slightly lower values of total detritus production and export compared to the FREE simulation, (a reduction of 6% and 20% respectively) . Although OFF simulations have lower average appendicularian biomass on an annual scale (see Fig. 4), their biomass is higher in spring during the phytoplankton bloom. This feature, combined with the higher primary production, explains why FREE and OFF simulations produce similar fluxes.

To assess the role of the three species potentially present at DyFAMed (*Oikopleura longicauda, dioica*, and *fusiformis*) three simulations with set biomass (OFF) were also conducted with the parameters given in the Appendix and derived from Lombard et al (2010). As summarized in Table 3,. the differences in the filtration, respiration and ingestion rates and the contrasting assimilation efficiencies produce clear changes in the fluxes: *O dioica* produces about half the detritus of *O longicauda,* while *O fusiformis* and *O longicauda* are comparable.

To investigate the response of appendicularian fluxes to phytoplankton biomass, simulations with lower and higher initial nitrate concentrations were conducted (Table 4). The variations of the initial nutrient content were meant to reflect the variability of winter hydrological conditions. For a 30% lower and higher initial nitrate, export from appendicularia varied weakly from 0.9 to 1.2 gC/m^2/yr, about -11% and +14% while total export varied to a larger extent (-12% and +19% respectively).

Finally, we performed a more general parameter sensitivity analysis by changing parameter values one at a time. Secondary production, detritus production and ammonium excretion fluxes from appendicularians are weakly sensitive to variations in appendicularian growth parameters (not shown). Overall, the response to a 10% variation in parameter values was linear and close to or lower than identity. The most sensitive parameters were the maximum filtration rate, the half

saturation constant for filtration and the respiration rate.

Discussion

The focus of our one-dimensional experiment was to obtain a reasonable description of the appendicularian environment, namely the seasonal cycle of prey and predator biomass, and temperature. Over the year 2000, Chl concentration agreed with observation, except during March when the Chl peak was overestimated compared to observations (up to 120 mg/m^2 instead of 60 mg/m^2). However, peaks of 100mg/m^2 were recorded during other years (in 1999, Marty et al 2002) and could have been missed in 2000 by the monthly frequency sampling.

In February-March, the model could not explain the observed drawdown of nitrate because mixed layer depth is equal to 200 m, preventing phytoplankton growth in the model. Synchronous with the nitrate drawdown, high Chl was observed in February, indicating that the bloom already started. Two possible mechanisms may be suggested: i) the bloom was immediately followed by a deep mixing event or ii) Chl-rich, nutrient-poor waters were advected at the DyFAMed station from the Ligurian current (e.g. Stemmann et al 2008). Both processes cannot be accounted for with a one dimensional model, unless higher resolution atmospheric forcings and additional physical data are provided.

Microzooplankton and HNAN biomass was overestimated in April-May, partly because of the high phytoplankton biomass. Since the biomass estimates are not from the same year as Chl measurements and taking into account the sparse sampling, further data are needed to explain the source of this overestimation. Spring nanozooplankton biomass was also overestimated by Raick et al (2005). The simulated net primary production (NPP) was in the lower range of in situ and satellite estimates, that have a large span due to different methods and to the large interannual variability (Marty and Chiaverini 2002).

Considering the delay in the phytoplankton peak timing as the main discrepancy, but given that Chl and zooplankton biomass were within the range of observations and comparable to previous studies (Raick et al 2005), this simulation was considered to be more than adequate to be used to assess the impact of appendicularians on the planktonic food web.

Typical in situ conditions at DyFAMed (Fig. 2, food generally lower than 100 mgC/m^3 and

T<25°C) are favorable for appendicularian growth. The higher HNAN growth rate indicates that they are better competitors for picophytoplankton than appendicularians.

The model predicts that appendicularian grazing impact is generally low, being about 1-4% of net primary production. This agrees well with other studies in mesotrophic environments (Tomita et al 1999). In contrast, appendicularians produce 3.9 gC/m^2/yr of large detritus, leading to an increase of 2.3 gC/m^2/yr in the simulated export flux at 200m. The inclusion of appendicularians generates an increase in detritus production independent of the mortality used, ranging from 2 % (OFF simulation) to 8% (FREE simulation). As most of this detritus sinks rapidly, this production translates into an increase in export flux from 23% to 55% respectively. *O dioica* is likely to produce about half the export of *O longicauda* and *O fusiformis*. Therefore, in absolute terms on an annual scale, appendicularian contribution to detritus production is low, but their contribution to export is considerable. The ratio of appendicularian detrital production to biomass is much greater than that of copepods (respectively 468 and 64), even higher than the production/biomass ratio (respectively 394 and 51), thus appendicularians are much more efficient than copepods at generating detritus. Appendicularians also produce fast sinking detritus which contains bacteria, picophytoplankton and HNAN inside particles, while that of the traditional route is simply predation of microphytoplankton by copepod. Appendicularians can also produce fast sinking detritus in an ecosystem dominated by small-sized particles (e.g., picoplankton).

Including appendicularians in the food web produces an export rate that is 44% higher than the value derived from sediment trap data (6.5 vs 4.5 gC/m^2/yr). Values of appendicularian-mediated export exceeding sediment trap estimates have been reported in several studies (e.g. Deibel et al 2005). This discrepancy can be attributed to several causes. First, the efficiency of the sediment trap for collecting appendicularian houses is probably poor due to their stickiness (Lombard et al 2010). However, the trapping efficiency of the DyFAMed trap was recently quantified as ca 100% from thorium isotope measurements (Roy-Barman et al 2009). More importantly, the degradation rate of houses and fecal pellets may be higher than the value used here (0.2/day), which is already in the upper range of estimates (Ploug et al 2008). In the model, a degradation rate of 0.7/day is sufficient to lower the total export to 4.5 gC/m^2/yr. High degradation was also reported by Vargas et al (2002), who observed a 70% loss of appendicularian houses between 10 m and 30 m. This high degradation possibly results from a combination of bacterial activity (Ploug et al 2008) and microzooplankton grazing (Poulsen and Iversen 2008). Thus, a better quantification of these two processes is needed to translate the appendicularian detritus flux into export.

Appendicularians produce detritus as fecal pellets and houses. Here we compare the simulated production of detritus (fecal pellets plus houses) to the only available estimate in the DyFAMed region (Point B), and as a further comparison to the only two other studies from other mesotrophic stations: the Sea of Japan (Tomita et al 1999), and Gullmar Fjord, Sweden (Vargas et al 2002). All the other studies on detritus production available in the literature are from coastal and eutrophic environments that are very different from DyFAMed (Taguchi 1982; Uye and Ichino 1995; Bauerfeind et al 1997; Hopcroft and Roff 1998; Dagg and Brown 2005b; Deibel et al 2005).

At Point B, a coastal station located 50 km from DyFAMed, Alldredge (2005) estimated a house-related carbon flux of 26 mgC/m^2/day at 75 m in May. This value is higher than the detritus flux simulated at 75 m, ranging from 5 mgC/m^2/yr (*O dioica*, OFF) to 11 mgC/m^2/day (*O longicauda*, OFF). OFF simulations were used for comparison as biomass in May was overestimated in the FREE simulations. The house flux estimated by Alldredge (2005) represented 32% of total export production. The model predicted it to be 5 and 10% of total detritus production for *O dioica* and *O longicauda* respectively. The lower contribution to export was partly due to (i) the higher simulated total export (113 against 82 mgC/m^2/day, estimated by Alldredge (2005) from the export at 200 m) and (ii) the method used by Alldredge (2005), omitting house weight loss.

In the Sea of Japan, Tomita et al (1999) estimated 2.66 mgC/m^3/day as the maximum house carbon production using a fraction of biomass production. We simulated a maximum detritus production of 1 mgC/m^3/day, 37% of the value of Tomita et al (1999). For the same station, Alldredge (2005) found a larger maximum house production for *O longicauda* of 7.2 mgC/m^3/day, computed using a size dependent house carbon content. This higher value probably came from the omission of house weight loss in the author's method. On an annual scale, the simulated detritus production was 3.9 gC/m^2/yr at DyFAMed, ca. one third of the house production rate of 11.3 gC/m^2/yr from Tomita et al (1999) in the Sea of Japan. This difference may be partly due to the lower simulated biomass compared to Tomita et al (1999) (18 against 25 mgC/m^2/yr), and to the high house carbon content taken by Tomita et al (1999).

In Gullmar Fjord, Vargas et al (2002) estimated appendicularian detritus fluxes from sediment traps in October and March. They found 19 mgC/m^2/day from *O dioica* detritus (pellets and houses) at 30m in October, with a biomass of ca 7 mgC/m^2. The maximum simulated export at DyFAMed was only 6 mgC/m^2/day at 30m depth in May (simulation OFF) with a biomass of 18 mgC/m^2 of *O dioica*. The values of Vargas et al (2002) of export relative to biomass may be due to the fairly high carbon content used (15.3% of body carbon) for houses, omitting weight loss after discard, and to

favorable food conditions with a maximum close to the surface. Comparison with March sampling in Vargas et al (2002) was not possible since *Fritillaria*, not included in our simulations, was dominant.

Therefore, our estimates of export rates are about 40% of the observational estimates of Alldredge (2005) at DyFAMed, probably because of an overestimation by the Alldredge (2005) method. Compared to the more mesotrophic sites of the Sea of Japan and Gullmar Fjord, our estimates are 60% lower. These lower estimates may simply be the response to lower food, i.e. the oligotrophic nature of the DyFAMed site. However, it may be that fluxes estimated with simple methods based on average house production rates and average carbon content result in overestimation. Regardless, appendicularian contribution to detritus production and export is significant but may be lower than previously estimated at the DyFAMed oligotrophic site, and it is lower than that estimated in mesotrophic environments.

The simulated impact of appendicularians depends on the biomass estimate. At DyFAMed, appendicularian biomass was 0-50 mgC/m^2, in the range of values reported in other comparable studies (80 mgC/m^2 Båmstedt et al 2005, 25.6 mgC/m^2 Tomita et al 1999, 3-6 mgC/m^2 Vargas et al 2002). This represented an average 0.8% (range 0 – 16%) of total mesozooplankton biomass. This proportion is consistent with other studies in mesotrophic environments (1.4%, range 0 – 5% Båmstedt et al 2005; 1.4% Tomita et al 1999; 1 to 4% Grice and Reeve 1982). However, the standard deviation of our biomass estimate is large (estimated here as the coefficient of variation std/mean = 140%), due to the high standard deviation in both abundance and mean weight estimates. In the range of possible values, we have chosen a rather large mean weight (2.23 µgC/ind) to compensate for the undersampling of small individuals (López-Urrutia et al 2005).

In the FREE simulation, a large mortality rate (0.02/day for linear and 0.1 mgC/m^3/day for density dependent) had to be imposed in order to keep appendicularian biomass to a realistic level during summer. This approach is validated by the similar fluxes obtained with simulations OFF where mortality is not included. High predation mortality is consistent with our knowledge of appendicularian ecology. Since they have no escape strategy, no vertical migration capability, and because of their high nutritional value (no hard parts as compared to copepods, which implies a higher nitrogen content per individual), appendicularia are potentially preferred prey for fish larvae and gelatinous carnivores (Gorsky and Fenaux 1998). However this approach has the drawback of limiting the time window of appearance of appendicularians compared to observations, and to be site-specific, i.e. the chosen mortality rates may be not apply in other regions. These drawbacks

suggest another approach, e.g. to parameterize appendicularians instead of actually representing them. If estimates of appendicularian biomass are available, one simple idea is to take their biomass as an input to the model. Then the fluxes would be computed as in the present study with null mortality, and setting the source-minus-sink term to zero at each time step. Thus their effect would simply be a transformation of their prey biomass into detritus, and ammonium, and matter would be conserved. If biomass estimates are not available, one could try a more simplistic, (though risky) approach, such as setting their biomass to a fixed fraction of other groups' biomass. However, before using this oversimplistic approach, study of appendicularians biomass in other time series stations such as BATS and HOT would be a necessary step for a more robust parameterization that can be applied at the global scale.

Considering our results in the framework of biogeochemical simulations for the global ocean, appendicularians appear to be a significant source of vertical carbon flux in most environments (Lombard et al 2010), and therefore are good candidates for a new plankton functional type *sensu* Le Queré et al (2005). Present biogeochemical models probably under, or misestimate, the production and export of detritus by only representing the pathway from large phytoplankton, copepods and detritus, omitting the picophytoplankton/HNAN-appendicularians-fast detritus pathway. This omission is probably serious in systems or seasons in which production is dominated by the picoplankton. However, including appendicularian effects on particulate flux also requires including the processes responsible for the transformation of this flux. Additional study of bacterial degradation and grazing by microzooplankton associated with appendicularian detritus (e.g. Poulsen and Iversen 2008) is critically needed.

Conclusion

Our ecosystem model including appendicularians suggests that in an oligotrophic environment such as DyFAMed, appendicularians are responsible for up to 8% of previously neglected detrital production, which translates into an increase of the export flux of carbon of up to 55% using conservative sinking rates. These results suggest that present biogeochemical models probably under, or misestimate the detritus and export production by neglecting the pathway from small size plankton to fast sinking detritus produced by appendicularians. The simulated yearly export exceeds by 44% sediment trap estimates, suggesting that their detritus degrades rapidly, as observed in other studies. Thus, although appendicularians appear to be efficient detritus producers, further work is needed to quantify the mechanisms and rates by which their detritus is degraded and grazed. Furthermore, for a comprehensive estimation of particulate export fluxes, winter appendicularian

species (*Fritillaria spp*), as well as salps and doliolids should be considered. As new ecophysiological knowledge is obtained from laboratory experiments, new organisms should be included in models and their biogeochemical significance assessed as in the present study if realistic ecosystems models are to be developed.

Acknowledgments

Authors acknowledge the DyFAMed observation system, the “Cellule piège”, Fabrizio d’Ortenzio for useful discussions, Franck Prejger and the Service RadeZoo. John Dolan is thanked for proofreading. This research was supported by the SESAME project, EC Contract No GOCE-036949, funded by the European Commission's Sixth Framework Programme under the priority 'Sustainable Development, Global Change and Ecosystems'.

Appendix: Model parameters

Appendicularian parameters

Parameter	Symbol	Unit	*O dioica*	*O longicauda*	*O fusiformis*	*Reference*
Q10 filtration	$t10_f$	-	1.06	1.10	1.09	1
Q10 respiration	$t10_r$	-	1.087	1.15	1.1	1
Maximum filtration rate	f	day^{-1}	3.0	8.0	7.0	1
Maximum respiration rate	f_r	day^{-1}	0.108	0.048	0.14	1
Preference micro-, nano- and pico-phytoplankton,	δ	-	0.0,0.5,1.0	0.0,0.5,1.0	0.0,0.5,1.0	Set
Preference bacteria, microzooplankton, HNAN			1.0,0.5,1.0	1.0,0.5,1.0	1.0,0.5,1.0	
Linear mortality	m	day^{-1}	0.02	0.05	0.06	Set
Density dependent mortality	m_{dns}	$mgC\ m^{-3}\ day^{-1}$	0.1	0.11	0.3	Set
Half saturation for filtration	K_f	$mgC\ m^{-3}$	150	518	300	1
Half saturation for ingestion efficiency	K_β	$mgC\ m^{-3}$	200	150	120	1
Half saturation for assimilation efficiency	K_η	$mgC\ m^{-3}$	130	120	300	1
Minimum ingestion efficiency	β_m	-	0.15	0.01	0.01	1
Minimum assimilation efficiency	η_m	-	0.10	0.01	0.1	1
C:N ratio	$R_{C:N}$	$gC\ molN^{-1}$	0.021	0.021	0.021	2
Fraction of house going to fast detritus	α_h	-	0.85	0.85	0.85	3
Sinking rate slow detritus	v^{sed}_{SD}	$m\ day^{-1}$	1.5		1.5	4
Sinking rate fast detritus copepod	v^{sed}_{FD}	$m\ day^{-1}$	5.0	5.0	5.0	5
Sinking rate fast detritus appendicularians	v^{sed}_{FD}	$m\ day^{-1}$	40.0	40.0	40.0	3

Table 1: Symbols, values and description of the appendicularians parameters. 1= Lombard et al (2010), 2=Gorsky et al (1988), 3=Lombard and Kiørboe (2010), 4=Lacroix and Nival (1998), 5=Lacroix and Grégoire (2002). Set : estimated from model trials in the range of literature values.

Modified parameters

In addition to appendicularians parameters, the model parameters departing from Vichi et al (2007) are given. Values identical to Vichi et al (2007) are noted 'std'.

Symbol	*P(1)*	*P(2)*	*P(3)*	*Description*	*Reference*
*r*0*P*	2.50	3.00	3.50	Maximum specific photosynthetic rate (d−1)	Raick et al (2005)
γ*P*	0.15	0.25	0.20	Activity respiration fraction (-)	Raick et al (2005)
bP	0.03	0.05	0.07	Basal respiration (d−1)	Raick et al (2005)
β*P*	std	0.10	0.10	Excreted fraction of primary production (-)	Spitz et al (2001)
W*sink P*(1)	0.00	-	-	Maximum sedimentation rate (m d−1)	Set
α_0 *chl*	0.9 10−5	1.3 10−5	1.1 10−5	Initial slope of PE curve i.e. maximum light utilization coefficient (mgC (mg chl)−1 μE−1 m2)	Geider et al (1997)
θ_0 *chl*	0.03	0.025	0.03	Optimal chl:C quotum (mg chl mg C−1)	Geider et al (1997)
cP	0.02	0.02	0.02	Chl-specific light absorption coefficient (m2 (mg chl)−1)	Raick et al (2005)

Table 2: Symbols, values and description of the phytoplankton parameters. *P*(1)= diatoms; *P*(2)= nanoflagellates, *P*(3)= picophytoplankton. Set : estimated from model trials in the range of literature values.

Symbol	*Z(4)*	*Z(5)*	*Z(6)*	*Description*	*Reference*
μZ	std	10.0	30.0	Feeding threshold (mg C m−3)	Set
*r*0*Z*	1.2	2.50	std	Potential specific growth rate (d−1)	Raick et al (2005)
vZ	0.05	-	-	Specific search volume (m3 mg C −1)	from Broekhuizen et al (1995)
bZ	0.001	0.01	0.03	Basal specific respiration rate (d−1)	Set
*d*0*Z*	0.01	0.01	0.03	Specific mortality rate (d−1)	Set
ddns Z	0.0004	-	-	Density-dependent specific mortality rate (m3 mgC−1 d−1)	Set
g*Z*	2.00	-	-	Exponent for density dependent mortality (-)	Set

Table 3: Symbols, values and description of the zooplankton parameters. *Z*(4)= mesozooplankton (copepod); *Z*(5)= microzooplankton; *Z*(6)=Heterotrophic nanoflagellates. Set : estimated from model trials in the range of literature values.

Symbol	*Value*	*Description*	*Reference*
*Q*10*B*	2.0	Characteristic Q10 coefficient	Raick et al (2005)
$\nu^1{}_B$	0.01	Specific potential *R*(1) uptake (d−1)	Set
$\nu^6{}_B$	0.08	Specific potential *R*(6) uptake (d−1)	Set
$\nu^8{}_B$	0.08	Specific potential *R*(8) uptake (d−1) (copepod fast detritus)	Set

v^{8}_{B}	0.2	Specific potential *R*(8) uptake (d−1) (appendicularians fast detritus)	Set

Table 4: Symbols, values and description of the Bacterioplankton parameters. Note that R(6) is slow detritus and R(8) is fast detritus. Set : estimated from model trials in the range of literature values.

Symbol	***Value***	***Description***	***Reference***
Λ^{nit}_{N4}	0.03	Specific nitrification rate (d−1)	Raick et al (2005)
h^{o}_{N4}	0.0	Half saturation oxygen concentration for chemical processes (mmolO2 m−3)	Set
λ_W	0.06	Optical extinction coefficient for pure water (m−1)	from Lacroix and Grégoire (2002)

Table 5: Symbols, values and description of the general pelagic parameters. Set : estimated from model trials in the range of literature values.

References

Aksnes, C. Troedsson and E.M. Thompson, (2006) Integrating developmental clocking and growth in a life-history model for the planktonic chordate *Oikopleura doica. Mar. Ecol., Prog. Ser.* **318**, 81–88.

Alldredge, A. L. (1981) The impact of appendicularian grazing on natural food concentrations in situ. *Limnol. Oceanogr.* **26,** 247–257

Alldredge, A.L. and Madin.L P (1982) Pelagic tunicates: unique herbivores in the marine plankton. *Bioscience,* **32**, 655-663

Alldredge, A. L. (2005) The contribution of discarded appendicularian houses to the flux of particulate organic carbon from oceanic surface waters, p. 309-326. In G. Gorsky, M. J. Youngbluth and D. Deibel [eds.], Response of marine ecosystems to global change: Ecological impact of appendicularians. GB Scientific Publisher.

Andersen, V., Nival, P. & R.P. Harris, (1987) Modelling of a planktonic ecosystem in an enclosed water column. *J. Mar. Biol. Ass. U.K.* **67**, 407-430.

Aumont, O., E. Maier-Reimer, S. Blain, and P. Monfray, (2003) An ecosystem model of the global ocean including Fe, Si, P colimitations, *Global Biogeochem. Cycles*, **17**, 1060, doi:10.1029/2001GB001745

Båmstedt, U., Fyhn, H.J., Martinussen, M.B., Mjaavatten, O., Grahl-Nielsen, O. (2005) Seasonal distribution, diversity and biochemical composition of appendicularians in Norwegian fjords. Pp. 233-259 in: G. Gorsky, M. Youngbluth (Eds.) Response of marine ecosystem to global change: Ecological impact of appendicularians. GB Scientific Publisher

Båmstedt U., Chemical composition and energy content. (1986) In: E.D.S. Corner and S.C.M. O'Hara, Editors, *The Biological Chemistry of Marine Copepods*, Clarendon Press, Oxford (1986), pp. 1–58.

Bauerfeind, C. Garrity, M. Krumholz, R.O. Ramseier and M. Voß, (1997) Seasonal variability of sediment trap collections in the Northeast Water Polynya. Part 2. Biochemical and microscopic composition of sedimenting matter, *J. Mar. Syst.* **10**, 371–389

Baretta J.W. et al (1995) The European-Regional-Seas-Ecosystem-Model, *Neth. J. Sea Res.* **33**, 233–246

Baretta-Bekker J.G., Baretta J.W., and W. Ebenhoeh. (1997) Microbial dynamics in the marine ecosystem model ERSEM II with decoupled carbon assimilation and nutrient

uptake. *J. Sea Res.*, **38,** 195–212

Bienfang, P. K. (1980) Herbivore diet affects fecal pellet settling. *Can. J. Fish. aquat. Sci*. **37**, 1352-1357

Broekhuizen, N., Heath, M.R., Hay, J.S., Gurney, W.S., (1995) Modelling the dynamics of the North Sea's mesozooplankton. *Neth. J. Sea Res.* **33**, 381-406.

Burchard, H., K. Bolding, and M. R. Villarreal, (1999) GOTM - a general ocean turbulence model. Theory, applications and test cases, *Tech. Rep. EUR 18745 EN*, European Commission

Carniel, S., Sclavo, M., Vichi, M., (2007) Sensitivity of a coupled physical-biological model to turbulence: High-frequency simulations in a northern Adriatic station. *Chemistry and Ecology*, **23,** 157-175, DOI: 10.1080/02757540701197903

Flood PR, Deibel D, Morris C (1992) Filtration of colloidal melanin from seawater by planktonic tunicates. *Nature* **355**, 630–632

Dagg M.J. and Brown S.L. (2005a) Clearance and ingestion rates of three appendicularian species, *Oikopleura longicauda, O. rufescens,* and *O. fusiformis*, In G. Gorsky, M. J. Youngbluth and D. Deibel [eds.], Response of marine ecosystems to global change: Ecological impact of appendicularians. GB Scientific Publisher.

Dagg M.J. and Brown S.L. (2005b) The potential contribution of fecal pellets from the larvacean *Oikopleura dioica* to vertical flux of carbon in a river dominated coastal margin, p. 293-308. In G. Gorsky, M. J. Youngbluth and D. Deibel [eds.], Response of marine ecosystems to global change: Ecological impact of appendicularians. GB Scientific Publisher.

Deibel. D, P.A. Saunders, J.L. Acuña, A.B. Bochdansky, N. Shiga and R.B. Rivkin, (2005) The role of appendicularians tunicates in the biogenic carbon cycle of three arctic Polynyas, p. 327-358. In G. Gorsky, M. J. Youngbluth and D. Deibel [eds.], Response of marine ecosystems to global change: Ecological impact of appendicularians. GB Scientific Publisher.

D'Ortenzio, F., D. Antoine and S. Marullo (2008) Satellite-driven modelling of the upper ocean mixed layer and air-sea CO2 flux in the Mediterranean Sea. *Deep-Sea Research* I, **55**, 405-434.

Edwards AM and Brindley J (1999) Zooplankton mortality and the dynamical behaviour of plankton population models. *Bull. Math. Biol.*, **61**, 303-339

Edwards, A. M. and Yool, A. (2000) The role of higher predation in plankton population models. *J. Plankton Res*. **22**, 1085–1112

Fasham M.J.R., Ducklow, H.W., McKelvie S.M, (1990) A nitrogen-based model of plankton dynamics in the oceanic mixed layer. *J. Mar. Res*. **48**, 591-639.

Fenaux, (1961) Existence d'un ordre cyclique d'abondance relative maximale chez les Appendiculaires de surface (Tuniciers pélagiques). *C.R. Acad. Sci.*, **253**, 2271-2273

Fyhn et al (2005) Amino and fatty acids in *Oikopleura dioica* pp. 171-188 in: G. Gorsky, M. Youngbluth (Eds.) Response of marine ecosystem to global change: Ecological impact of appendicularians. GB Scientific Publisher

Gasparini, S; Mousseau, Laure; Marty, Jean-Claude (2004) Zooplankton biomass at DYFAMED time series station. doi:10.1594/PANGAEA.183618

Geider, R. J., H. L. MacIntyre and T. M. Kana. (1997) A dynamic model of phytoplankton growth and acclimation: responses of the balanced growth rate and the chlorophyll *a*:carbon ratio of light, nutrient-limitation and temperature. *Mar. Ecol. Prog. Ser.* **148**, 187-200

Gorsky, G., Fisher, N. S., Fowler, S. W. (1984) Biogenic debris from the pelagic tunicate, Oikopleura dioica, and its role in the vertical transport of a transuranium element. *Estuar Coast. Shelf Sci*. **18**, 13-23

Gorsky G., Dallot S., Sardou J., Fenaux R., Carré C., and Palazzoli I. (1988) Carbon and nitrogen composition of some northwestern Mediterranean zooplankton and micronekton. *J. Exp. Mar. Biol. Ecol.*, **124**, 133-144.

Gorsky, G., Fenaux R. (1998) The role of appendicularia in marine food webs,, in The biology of pelagic tunicates, Q Bone Ed, Oxford University Press, pp. 161-169.

Gorsky, G., Ohman, M.D., Picheral, M., Gasparini,S., Stemmann,L, Romagnan, J.-B, Cawood A, S Pesant S, Garcia-Comas C, Prejger, F., (2010) Digital zooplankton image analysis using the ZooScan integrated analysis system, *J. Plankton Res*. **32,**285-303

Grice G. D. and Reeve M. R. (1982) Marine mesocosms, Biological and Chemical Research in Experimental ecosystems. New York, Springer Verlag

Hay S.J., Kiørboe T. Matthews A., (1991) Zooplankton biomass and production in the North Sea during the Autumn Circulation Experiment, October 1987–March 1988, *Cont. Shelf. Res.* **11**, 1453–1476

Hopcroft, R.R. and Roff, J.C., (1998) Production of tropical larvaceans in Kingston Harbour, Jamaica: are we ignoring an important secondary producer? *J. Plankton Res.,* **20**, 557-569.

Lacroix, G., Grégoire, M., (2002) Revisited ecosystem model (MODECOGeL) of the Ligurian Sea: seasonal and interannual variability due to atmospheric forcing. *J. Mar. Syst.* **37**, 229–258.

Lacroix, G., Nival, P., (1998) Influence of meteorological variability on primary production dynamics in the Ligurian Sea (NW Mediterranean Sea) with a hydrodynamic/biological model. *J. Mar. Syst.* **16**, 23– 50.

Lazzari, P., A. Teruzzi, S. Salon, S. Campagna, C. Calonaci, S. Colella, M. Tonani, and A. Crise (2010) Pre-operational short-term forecasts for Mediterranean Sea biogeochemistry *Ocean Sci*., **6**, 25-39.

Le Quéré, C., S. P. Harrison, I. Colin Prentice, E. T. Buitenhuis, O. Aumont, L. Bopp, H. Claustre, L. Cotrim da Cunha, R. Geider, X. Giraud, C. Klaas, K. E. Kohfeld, L. Legendre, M. Manizza, T. Platt, R. B. Rivkin, S. Sathyendranath, J. Uitz, A. J. Watson, and D. Wolf-Gladrow, (2005) Ecosystem dynamics based on plankton functional types for global ocean biogeochemistry models. *Global Change Biol.*, **11**, doi:10.11111/j.1365-2486.2005.01004.x, 2016-2040.

Lévy, M., Mémery, L., and J.-M. André (1998) Simulation of primary production and export fluxes in the NW Mediterranean Sea, *J. Mar. Res.,* **56**, 197-238

Lombard F., Sciandra A., Gorsky G. (2005) Influence of body mass, food concentration, temperature and filtering activity on the oxygen uptake of the appendicularian *Oikopleura dioica*. *Mar. Ecol., Prog. Ser.*, **301**, 149-158.

Lombard F., Renaud F., Sainsbury C., Sciandra A., Gorsky G. (2009a) Appendicularians ecophysiology I. Food concentration dependent clearance rate, assimilation efficiency, growth, maturation and reproduction of *Oikopleura dioica*. *J. Mar. Syst.* doi:10.1016/j.jmarsys.2009.01.004

Lombard F., Sciandra A., Gorsky G. (2009b) Appendicularians ecophysiology II. Reproducing clearance, growth, respiration and particles production of the appendicularian *Oikopleura dioica* by modeling its ecophysiology. *J. Mar. Syst.* doi:10.1016/j.jmarsys.2009.01.005

Lombard F., Legendre L., Picheral M., Sciandra A., Gorsky G. (2010) Prediction of ecological niches and carbon export by appendicularians using a new multispecies ecophysiological model. *Mar. Ecol., Prog. Ser.*, **398**,109-125

Lombard, F., Eloire, D., Gobet, A., Legendre, L. Stemmann, L., Dolan, J.R., Sciandra, A., Gorsky, G. (2010) Experimental and modeling evidence of appendicularian-ciliate interactions. *Limnol. Oceanogr.*, **55**,77-90

Lombard, F. and Kiørboe, T. (2010) Marine snow originating from appendicularian houses: Age-dependent settling characteristics, *Deep-Sea Res.* I **57**, 1304-1313

López-Urrutia A. Acuña J.L., X. Irigoien and R. Harris, (2003) Food limitation and growth in temperate epipelagic appendicularians (Tunicata), *Mar. Ecol. Prog. Ser.* **252**, 143–157.

López-Urrutia, A., Harris R.P., Smith T. (2004) Predation by calanoid copepods on the appendicularian *Oikopleura dioica Limnol. Oceanogr.* **49**, 303-307

López-Urrutia, A., Harris, R.P., Acuña, J.L., Båmstedt, U., Flood, P.R., Fyhn, H.J., Gasser, B.,Gorsky, G., Irigoien, X., Martinussen, M.B., (2005) A comparison of appendicularians seasonal cycles in four distinct European coastal environments p. 255-276. In G. Gorsky, M. J. Youngbluth and D. Deibel [eds.], Response of marine ecosystems to global change: Ecological impact of appendicularians. GB Scientific Publisher.

Marty, J.-C. (2002) The DYFAMED time-series program (French-JGOFS). *Deep-Sea Res* II **49**, 1963– 1964

Marty, J.-C., and Chiaverini J. (2002) Seasonal and interannual variations in phytoplankton production at DYFAMED time-series station, northwestern Mediterranean Sea, *Deep-Sea Res.* II, **49**, 2017–2030.

Marty, J.C., Chiaverini, J., Pizay, M.D., Avril, B., (2002) Seasonal and interannual dynamics of phytoplankton pigments in the Western Mediterranean sea at the DYFAMED time-series station (1991-1999). *Deep-Sea Res* II **49**, 1965-1985

Miquel, J.-C., S. W. Fowler and J. La Rosa. (1993) Vertical particle fluxes in the Ligurian Sea. *Ann. Inst. Oceanogr*., **69***,* 107–110.

Miquel, J.-C., S.W. Flower, J. La Rosa and P. Buat-Menard. (1994) Dynamics of the downward flux of particles and carbon in the open Northwestern Mediterranean Sea. *Deep-Sea Res*, **41***,* 243–262.

Nakamura, Y., Suzuki, K., Suzuki, S. and Hiromi, J. (1997) Production of *Oikopleura dioica* (Appendicularia) following a picoplankton 'bloom' in a eutrophic coastal area. *J. Plankton Res.*, **19**, 113–124

Neumann, T., W. Fennel, and C. Kremp, (2002) Experimental simulations with an ecosystem model of the Baltic Sea: A nutrient load reduction experiment, *Glob. Biogeochem. Cycles*, **16**, 10.1029/2001GB001,450

Ploug H., Iversen, M., and Fischer, G. (2008) Ballast, sinking velocity, and apparent diffusivity within marine snow and zooplankton fecal pellets: Implication for substrate turnover by attached bacteria, *Limnol. Oceanogr.* **53**, 1878–1886

Polimene L., Pinardi N., Zavatarelli M., Allen J. I., Giani M., Vichi M. (2007) A

numerical simulation study of dissolved organic carbon accumulation in the northern Adriatic Sea. *J. of Geophys. Res.*, doi: 1029/JC003529.

Poulsen L.K. and Iversen M.H. (2008) Degradation of copepod fecal pellets: key role of protozooplankton. *Mar. Ecol. Prog. Ser.* **367**, 1-13

Raick C., Delhez E.J.M., Soetaert K., Gregoire M. (2005) Study of the seasonal cycle of the biological productivity in the Ligurian Sea using an 1D interdisciplinary model. *J. Mar. Syst.* **55**, 177-203.

Roy-Barman, M. C. Lemaître, Ayrault, S., C. Jeandel, M. Souhaut, J.-C. Miquel (2009) The influence of particle composition on Thorium scavenging in the Mediterranean Sea. *Earth Planet. Sci. Lett.* **286** 526–534

Sato R, Tanaka Y., Ishimaru T. (2005) Clearance and ingestion rates of three appendicularian species, *Oikopleura longicauda, O. rufescens*, and *O. fusiformis*, in G. Gorsky, M. Youngbluth (Eds.) Response of marine ecosystem to global change: Ecological impact of appendicularians. GB Scientific Publisher

Sommer F., T. Hansen, H. Feuchtmayr, B. Santer, N. Tokle, U. Sommer (2003) Do calanoid copepods suppress appendicularians in the coastal ocean? *J. Plankton Res*., **25**, 869-871

Spitz, Y.H., J.R. Moisan, M.R. Abbott, (2001) Configuring an ecosystem model using data from the Bermuda-Atlantic Time Series (BATS). *Deep-Sea Res.* II, **48**, 1733-1768.

Stibor H., Vadstein O., Lippert B., Roederer W., Olsen Y. (2004) Calanoid copepods and nutrient enrichment determine population dynamics of the appendicularian *Oikopleura dioica*: a mesocosm experiment. *Mar. Ecol. Prog. Ser,* **270**, 209-215

Stemmann L., Picheral M., Taupier-Letage I., Legendre L., Prieur L.,Guidi L., Gorsky G. (2008) Effects of frontal processes on marine aggregate dynamics and fluxes : an inter annual study in a permanent geostrophic front (NW Mediterranean). *J. Mar. Syst.,* **70**, 1-20

Taguchi S. (1982) Seasonal study of fecal pellets and discarded houses of Appendicularia in a subtropical inlet, Kaneohe Bay, Hawaii. *Estuar. Coast. Shelf Sci.,* **14**, 545–555

Tomita et al. (1999) Production of *Oikopleura longicauda* (Tunicata: Appendicularia) in Toyama Bay, southern Japan Sea, *J. Plankton Res*., **21**, 2421-2430

Touratier, F., Carlotti, F. and Gorsky, G., (2003) Individual growth model for the appendicularian *Oikopleura dioica*. *Mar. Ecol., Prog. Ser.,* **248**, 141-163.

Urban J.L., McKenzie CH. and Deibel JD. (1992) Seasonal differences in the content of *Oikopleura vanhoeffeni* and *Calanus finmarchicus* faecal pellets: illustrations of

zooplankton food web shifts in coastal Newfoundland waters. *Mar. Ecol. Prog. Ser.,* **84**, 255-264.

Urban J.L., Deibel J.D. and Schwinghamer P. (1993) Seasonal variations in the densities of fecal pellets produced by *Oikopleura vanhoeffeni* (C. Larvacea) and *Calanus finmarchicus* (C. Copepoda). *Mar. Biol.,* **117,** 607-613

Uye S., Ichino S. (1995) Seasonal variations in abundance, size composition, biomass and production rate of *Oikopleura dioica* (Fol) (Tunicata: Appendicularia) in a temperate eutrophic inlet. *J. Exp. Mar. Biol. Ecol.,* **189**,1–11

Vargas, C. A., K. Toennesson, A. Sell, M. Maar, E. F. Moeller, T. Zervoudaki, A. Giannakourou, E. Christou, S. Satapoomin, J. K. Petersen, T. G. Nielsen, and P. Tiselius. (2002) Importance of copepods versus appendicularians in vertical carbon fluxes in a Swedish fjord. *Mar. Ecol., Prog. Ser.,* **241**, 125-138.

Vichi M., N. Pinardi and S. Masina (2007) A generalized model of pelagic biogeochemistry for the global ocean ecosystem. Part I: Theory. *J. Mar. Syst.*, **64**, 89-109.

Vichi M., S. Masina (2009) Skill assessment of the PELAGOS global ocean biogeochemistry model over the period 1980–2000. *Biogeosciences*, **6**, 2333-2353

Vidussi F., H. Claustre, B.B. Manca, A. Luchetta, J.-C Marty, J. Chiavérini (2001) Phytoplankton pigment distribution in relation to upper thermocline circulation in the eastern Mediterranean Sea during winter. *J.Geophys. Res.,* **106** (C9), 19939–19956

Tables and Figures legends

Table 1: Simulations set up

Table 2: Main annual biogeochemical fluxes for simulation with no appendicularian (no-app), FREE appendicularian (app-free) and OFF appendicularians (app-off). In simulations OFF, the appendicularian biomass is set and an offline mortality term is computed. The slow detritus production corresponding to the offline mortality is reported in italics.

Table 3: Main annual biogeochemical fluxes for the three main appendicularian species (simulation app-off-species). In simulations OFF, the appendicularian biomass is set and an offline mortality term is computed. The slow detritus production corresponding to the offline mortality is reported in italics.

Table 4: Annual appendicularian biogeochemical fluxes for a ±30% variation of the nitrate initial conditions, simulations app-off-sens

Figure 1: Block diagram of the model. For clarity, arrows representing flow of NH_4, DOM, and detritus indicated in the legend are numbered and not connected. P1 is microphytoplankton, P2 is nanophytoplankton and P3 is picophytoplankton.

Figure 2: Net growth rate (day-1) as a function of food concentration and temperature for appendicularian *Oikopleura longicauda*, copepods, microzooplankton and Heterotrophic nanoflagellate (HNAN). Net growth is computed as the uptake minus egestion, excretion, respiration, defecation and mortality.

Figure 3: Annual time course of the mixed layer depth and 5 m depth temperature for the model (line) and the observations (triangles). Mixed layer depth observations are bounded at 200m, the bottom of the modeled domain.

Figure 4: Annual time course of simulations with and without appendicularians (solid line no-app, dashed line app-free) and observations (triangles), depth integrated over 0-200m except for bacteria and microzooplankton (5-110m, the sampled layer). In the copepod panel, triangles are data from 2001-2002 (Gasparini et al 2004) while circles are estimates from the present study (2006-2008). The set biomass used for simulations OFF (see section simulations set up) is drawn in the appendicularians panel as heavy dashed line.

Figure 5: Annual time course of net primary and secondary production (A) and export production at 200 m (B) for model (lines) and sediment traps (bars) for simulation without appendicularians (no-app).

Figure 6: Annual time course of net primary and secondary production (A) and export

production at 200 m (B) for model (lines) and sediment traps (bars) for simulation with appendicularians (app-free).

Figure 7: Annual contribution of each living group to the main biogeochemical fluxes, for run without appendicularians (no-app)

Figure 8: Annual contribution of each living group to the main biogeochemical fluxes, for run with appendicularians (app-free)

Simulations name	Appendicularians	Objective
No-app	No	Reference run
app-free	Yes, free biomass	Appendicularian impact
app-off	Yes, set biomass	Appendicularian impact without mortality
app-off-species	Yes, set biomass	Impact of different appendicularian species
app-off-sens	Yes, set biomass	Sensitivity to parameters and nitrate initial conditions

Table 1 : Simulations set up

Annual flux (gC/m^2/yr) *(mmolN/m^2/yr)	no-app	app-free	app-off
Net primary production	102.4	96.5	102
Export non App	4.2	4.0	4.1
Export App	-	2.4	1.0
Excretion NH4 App*	-	46.3	46.3
App uptake Phytoplankton	-	3.9	1.5
Other uptake Phytoplankton	69.8	60.5	67.7
App uptake MiZ+HNAN	-	3.5	1.5
App uptake Bac	-	4.6	2.3
Cop uptake App	-	0.9	0.3
MiZ+HNAN uptake Bac	32.2	24.2	29.0
Slow Detritus production total	35.2	37.3	35.1
Slow Detritus production App	-	4.5	0.5+*1.3*
Fast Detritus production total	16.6	18.7	17.6
Fast Detritus production App	-	3.9	1.4
Slow Detritus Export	1.1	1.2	1.2
Fast Detritus Export	3.1	5.3	3.9

Table 2 : Main annual biogeochemical fluxes for simulation with no appendicularian (no-app), FREE appendicularian (app-free) and OFF appendicularians (app-off). In simulations OFF, the appendicularian biomass is set and an offline mortality term is computed. The slow detritus production corresponding to the offline mortality is reported in italics

Annual flux ($gC/m^2/yr$)	*O longicauda*	*O dioica*	*O fusiformis*
Net primary production	102.0	102.4	102.7
Export non App	4.1	4.2	4.1
Export App	1.0	0.5	1.0
Slow Detritus production total	35.1	35.2	35.3
Slow Detritus production App	0.5+*1.3*	0.2+*0.6*	0.5+*1.7*
Fast Detritus production total	17.6	17.2	17.6
Fast Detritus production App	1.4	0.7	1.4
Slow Detritus Export	1.2	1.2	1.2
Fast Detritus Export	3.9	3.5	3.9

Table 3 : Main annual biogeochemical fluxes for the three main appendicularian species (simulation app-off-species). In simulations OFF, the appendicularian biomass is set and an offline mortality term is computed. The slow detritus production corresponding to the offline mortality is reported in italics.

Annual flux (gC/m^2/yr)	-30%	Control	+30%
Net primary production	83.3	102	117.4
Export non App	3.2	4.1	4.5
Export App	0.9	1.0	1.2
App uptake Phytoplankton	1.4	1.5	1.7

Table 4 : Annual appendicularian biogeochemical fluxes for a ±30% variation of the nitrate initial conditions, simulations app-off-sens

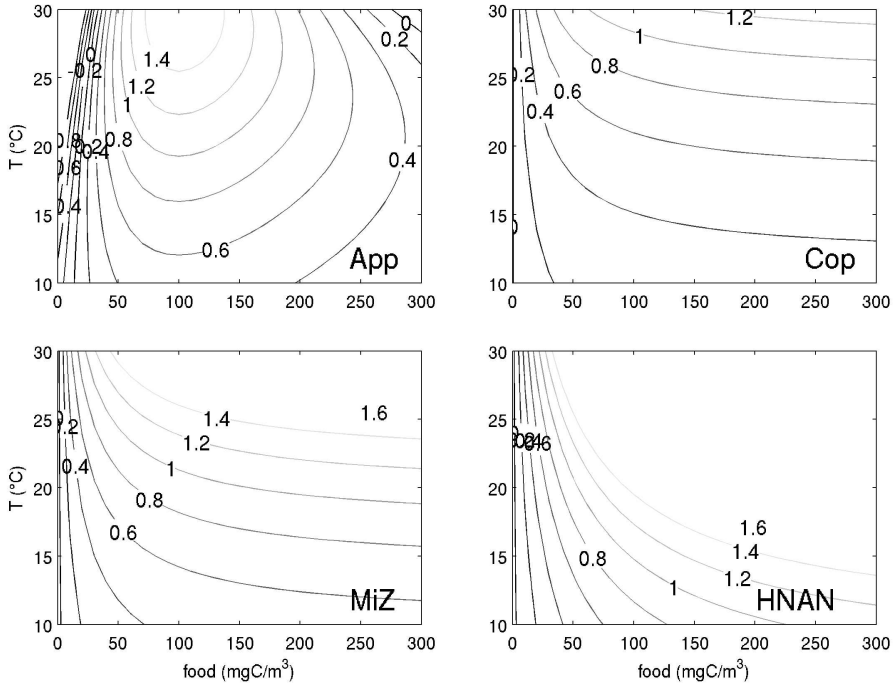

Net growth rate (day-1) as a function of food concentration and temperature for appendicularian Oikopleura longicauda, copepods, microzooplankton and Heterotrophic nanoflagellate (HNAN). Net growth is computed as the uptake minus egestion, excretion, respiration, defecation and mortality.
203x152mm (300 x 300 DPI)

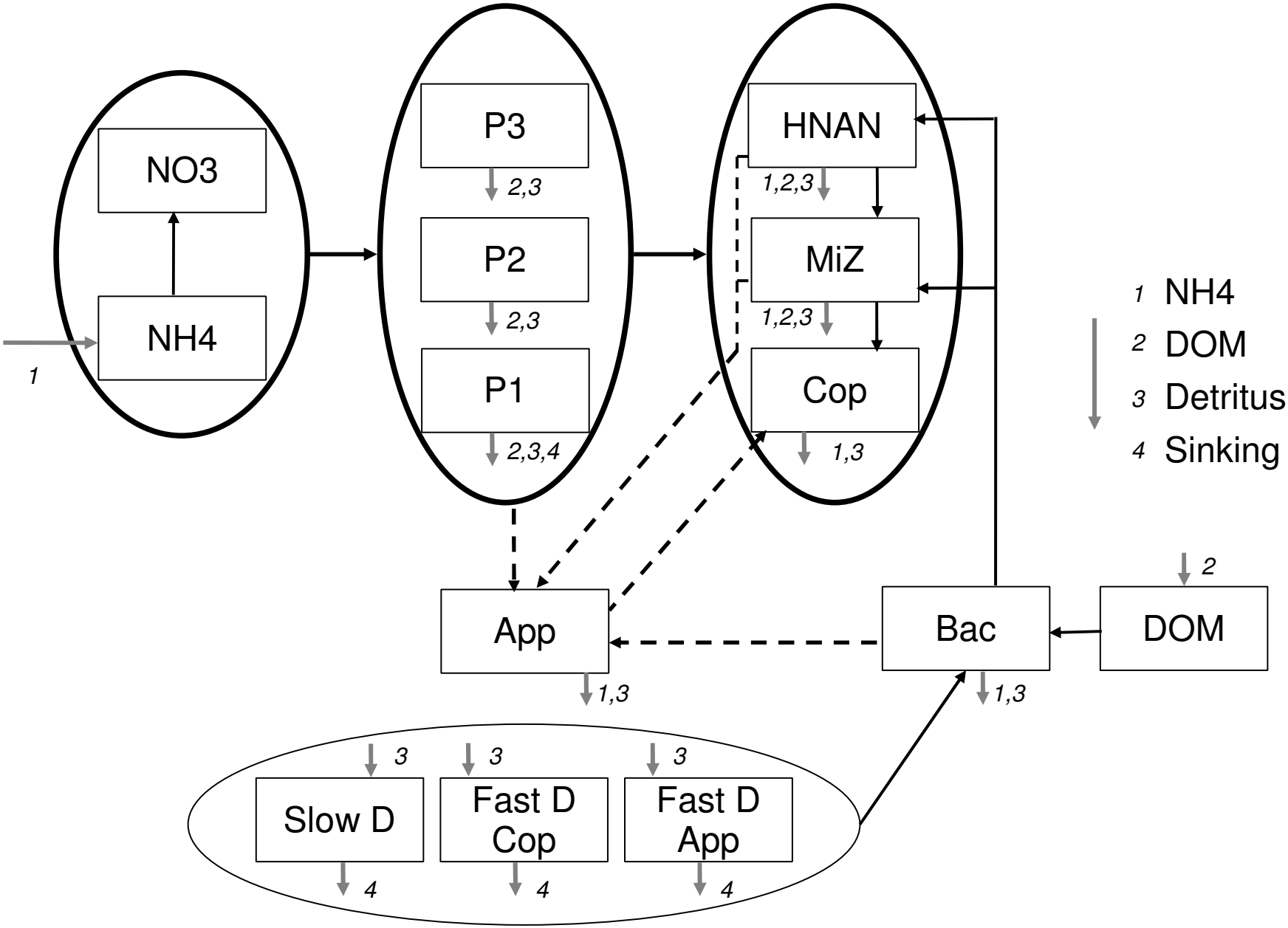
NO3
NH4
1
P3
2,3
P2
2,3
P1
2,3,4
HNAN
1,2,3
MiZ
1,2,3
Cop
1,3
1 NH4
2 DOM
3 Detritus
4 Sinking
App
1,3
Bac
1,3
2
DOM
3
3
3
Slow D
Fast D Cop
Fast D App
4
4
4

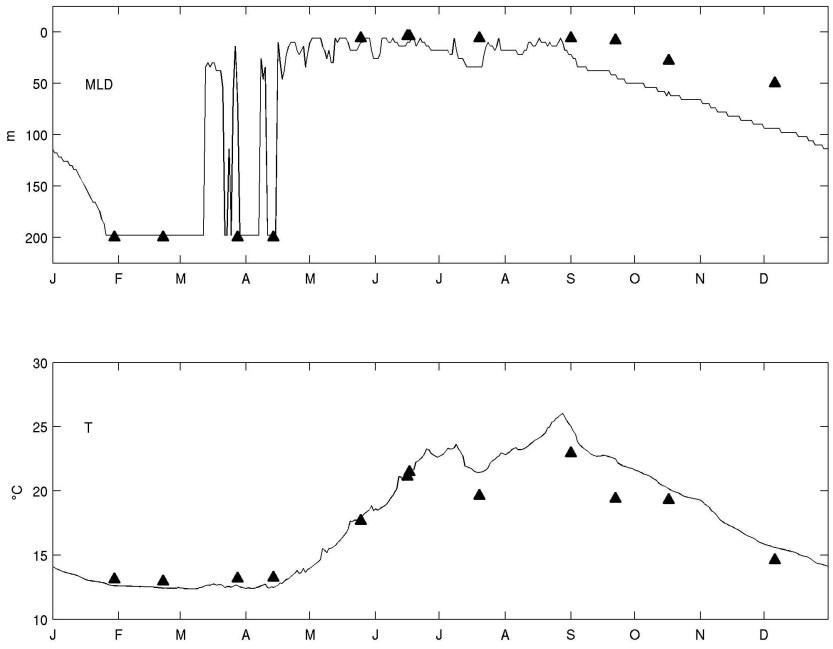

Annual time course of the mixed layer depth and 5 m depth temperature for the model (line) and the observations (triangles). Mixed layer depth observations are bounded at 200m, the bottom of the modeled domain.
203x152mm (300 x 300 DPI)

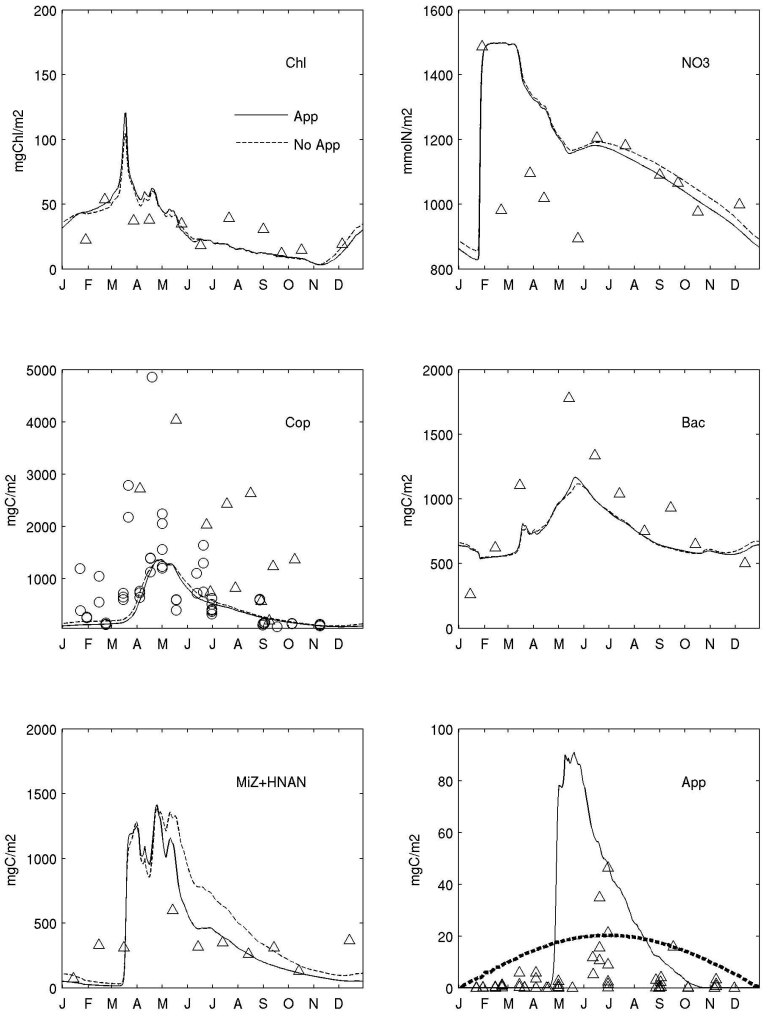

Annual time course of simulations with and without appendicularians (solid line no-app, dashed line app-free) and observations (triangles), depth integrated over 0-200m except for bacteria and microzooplankton (5-110m, the sampled layer). In the copepod panel, triangles are data from 2001-2002 (Gasparini et al 2004) while circles are estimates from the present study (2006-2008). The set biomass used for simulations OFF (see section simulations set up) is drawn in the appendicularians panel as heavy dashed line.
179x239mm (300 x 300 DPI)

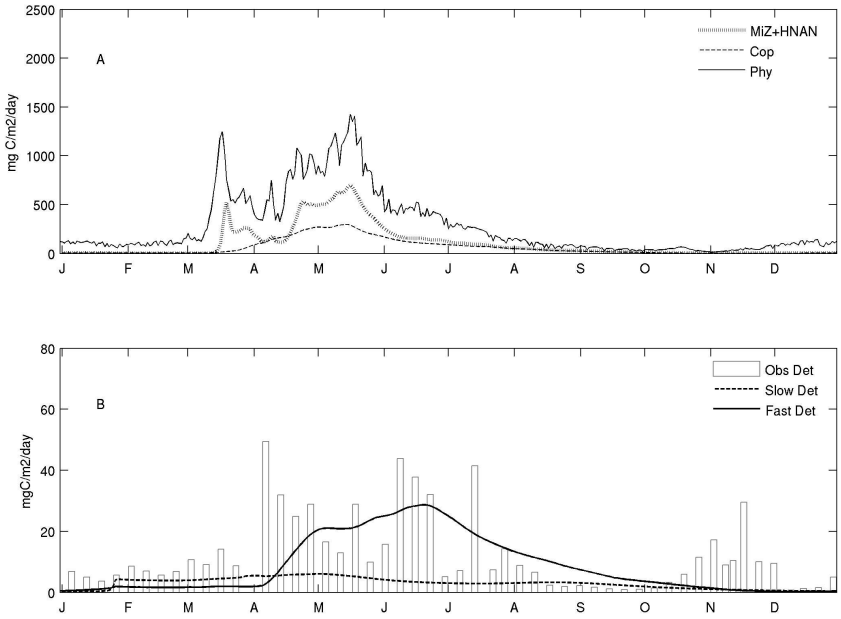

Annual time course of net primary and secondary production (A) and export production at 200 m (B) for model (lines) and sediment traps (bars) for simulation without appendicularians (no-app).
209x149mm (300 x 300 DPI)

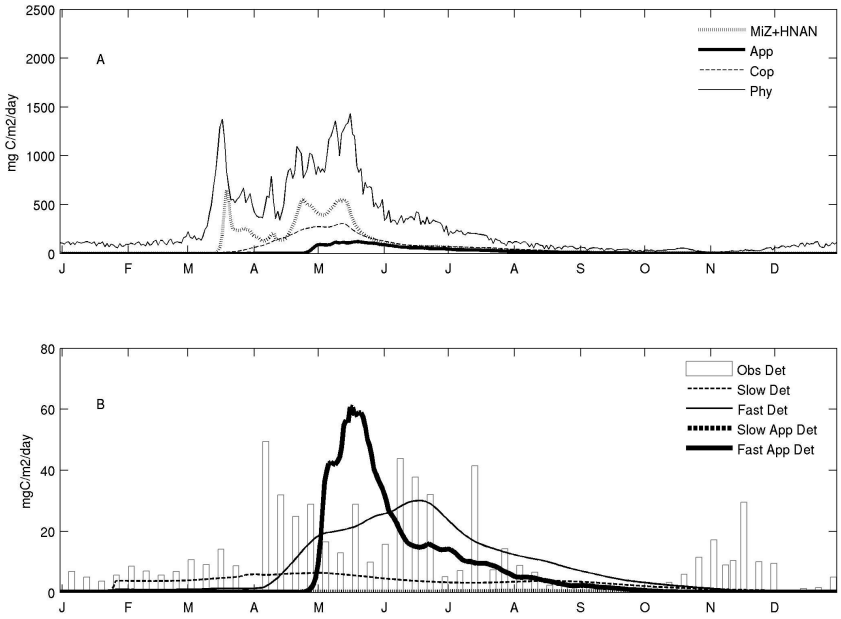

Annual time course of net primary and secondary production (A) and export production at 200 m (B) for model (lines) and sediment traps (bars) for simulation with appendicularians (app-free).
209x149mm (300 x 300 DPI)

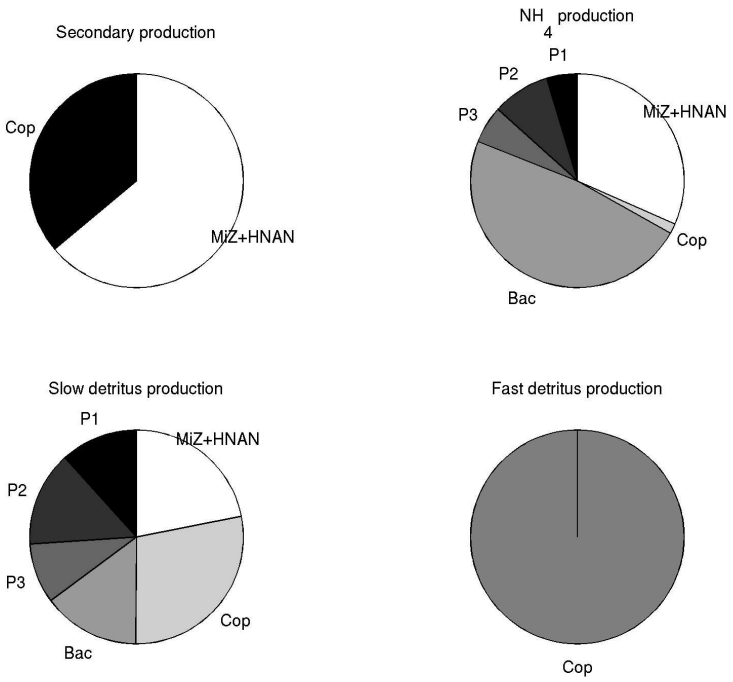

Annual contribution of each living group to the main biogeochemical fluxes, for run without appendicularians (no-app)
167x125mm (300 x 300 DPI)

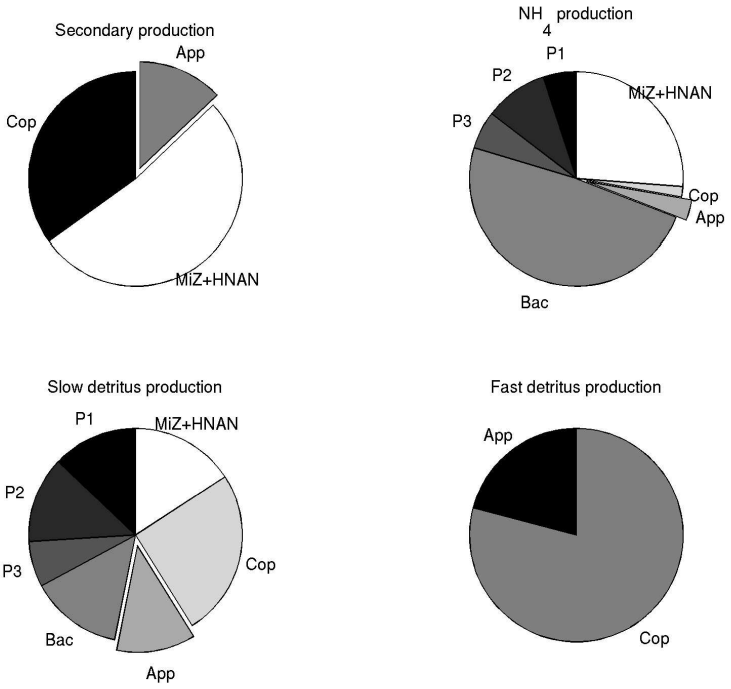

Annual contribution of each living group to the main biogeochemical fluxes, for run with appendicularians (app-free)
167x125mm (300 x 300 DPI)